Special issue article

SURFACE and INTERFACE ANALYSIS

Received: 13 October 2011 Accepted: 18 October 2011 Published online in Wiley Online Library: 12 January 2012

(wileyonlinelibrary.com) DOI 10.1002/sia.3861

Reflection electron energy loss spectroscopy for ultrathin gate oxide materials

Hye Chung Shin,[a] Dahlang Tahir,[b] Soonjoo Seo,[a] Yus Rama Denny,[a] Suhk Kun Oh,[a] Hee Jae Kang,[a]* Sung Heo,[c] Jae Gwan Chung,[c] Jae Cheol Lee[c] and Sven Tougaard[d]

The band alignment of $HfZrO_4$ gate oxide thin films on Si (100) deposited by the atomic layer deposition method has been investigated using reflection electron energy loss spectroscopy and XPS. The band gap of $HfZrO_4$ gate oxide thin film is 5.40 ± 0.05 eV. The valence band offset (ΔE_v) and the conduction band offset (ΔE_c) are 2.50 ± 0.05 eV and 1.78 ± 0.05 eV, respectively. These values satisfy the minimum requirement for the hole and electron barrier heights of larger than 1 eV for device applications. We have demonstrated that the quantitative analysis of reflection electron energy loss spectroscopy spectra obtained from $HfZrO_4$ thin films provides us a straightforward way to determine the optical properties and the inelastic mean free path of ultrathin gate oxide materials. **Copyright © 2012 John Wiley & Sons, Ltd.**

Keywords: electronic and optical properties; $HfZrO_4$ gate oxide thin film; REELS

Introduction

Reflection electron energy loss spectroscopy (REELS) is surface sensitive and capable of analyzing electronic and optical properties of ultrathin gate oxide materials because the low-energy-loss region reflects the valence and conduction band structures of solids. When the energetic electrons are impinging upon a solid, the incident electrons are inelastically scattered through interaction with either outer-shell or inner-shell atomic electrons.[1] Excitation of outer-shell electrons can result in an energy loss of less than 100 eV. It provides a straightforward way to obtain the dielectric function and, thereby, the electronic properties of a solid and to determine the inelastic scattering properties, which is important for surface electron spectroscopy analysis. The plasmon loss corresponds to a collective oscillation of the valence electron. The energy of the plasmon loss is related to the density of valence electron and is sensitive to the change in the band structure.

Recently, REELS has been successfully used to investigate ultrathin gate oxide materials adopted in CMOS.[2–6] Among the candidates of gate oxide materials in CMOS, Hf-based and Zr-based high-*k* gate dielectrics are highly promising and thus have been extensively studied.[2–7] We focused on how to obtain the band gap and the optical properties of ultrathin gate oxide materials through a quantitative analysis of REELS spectra obtained from $HfZrO_4$ thin films.

Within the view point of electron spectroscopy, the inelastic mean free path (IMFP) is a very important factor for surface analysis.[4–6] We demonstrated how to obtain the IMFP values from the REELS of the $HfZrO_4$ gate oxide thin film.

Experiment

$HfZrO_4$ thin films were grown on p-Si (100) substrate by alternating atomic layer deposition processes for HfO_2 and ZrO_2 contents in a controlled manner. Hence, the composition and the thickness of a thin film can be controlled by varying the number of cycles and deposition time for HfO_2 and ZrO_2 contents, respectively. The composition of thin films was confirmed by XPS quantification. Prior to growing oxide films, p-type Si substrates were cleaned by using the Radio Corporation of America method.[8] $Hf[N(CH_3)(CH_2CH_3)]_4$ and $Zr[N(CH_3)(CH_2CH_3)]_4$ were used as precursors for HfO_2 and ZrO_2, respectively. O_3 vapor was used as oxygen source. The thin films were grown in N_2 atmosphere supplied as the purge and carrier gas. The substrate temperature was kept below 300 °C during the thin film deposition. The physical thickness of the thin film was 7 nm. REELS spectra were obtained using the VG ESCALAB 210 with LaB_6 electron gun and recorded at a constant pass energy mode of 20 eV. The incident angle of primary electrons and the take-off angle of reflected electrons were 55° and 0° from the surface normal, respectively. XPS spectra were obtained with Mg Kα source (1253.6 eV) and pass energy of 20 eV. The binding energies were referenced to C 1s peak of hydrocarbon contamination at 285 eV. The primary electron energies were 1.0, 1.5 and 1.8 keV. The energy resolution, given by the full width at half maximum of the elastic peak of backscattered electrons, was approximately 0.8 eV and the energy loss range was measured up to 100 eV.

* *Correspondence to: Hee Jae Kang, Department of Physics, Chungbuk National University, Cheongju, 361–763, Korea. E-mail: hjkang@cbu.ac.kr*

a *Department of Physics, Chungbuk National University, Cheongju 361-763, Korea*

b *Department of Physics, Hasanuddin University, Makassar, 90245, Indonesia*

c *Analytical Engineering Center, Samsung Advanced Institute of Technology, Suwon, 440-600, Korea*

d *Department of Physics and Chemistry, University of Southern Denmark, Odense M. DK-5230, Denmark*

Copyright © 2012 John Wiley & Sons, Ltd.

Results and discussion

Figure 1 shows the REELS spectrum for $HfZrO_4$ gate oxide thin films. The band gap was determined from the onset of energy loss spectrum. The method was previously described in our papers.[2,3] The measured band gap for the $HfZrO_4$ gate oxide thin film was 5.40 eV. The valence band spectrum was measured to obtain the valence band offset at the dielectric/Si interface. The XPS valence band spectrum is shown in Fig. 2. The valence band maximum (VBM) was determined from the intersection of two lines, which met the linear fits of the valence band leading edge and the background. The valence band offset was obtained from the energy difference between the VBM of the gate dielectric and that of Si. The VBM of *p*-Si bulk is positioned at 0.24 eV. We do not take into account any possible band bending of silicon at the interface between the gate oxide thin film and the Si substrate. The valence band offset (ΔE_v) was 2.50 ± 0.05 eV. The band gap and the valence band offset allow us to determine the conduction band offset (ΔE_c) using the following expression:[2,3]

$$\Delta E_c = E_g(\text{oxide}) - E_g(\text{Si}) - \Delta E_v(\text{oxide/Si}). \quad (1)$$

Here, E_g (oxide) and E_g (Si) are the band gaps of an oxide thin film and silicon, respectively. ΔE_c of $HfZrO_4$ is 1.78 ± 0.05 eV. This value meets the requirement for electronic devices in which the barrier height is larger than 1 eV. Interestingly, our results show that the band gap, the valence band offset, and the conduction band offset of the $HfZrO_4$ are located midway between HfO_2 and ZrO_2, which is consistent with the literature.[3,5]

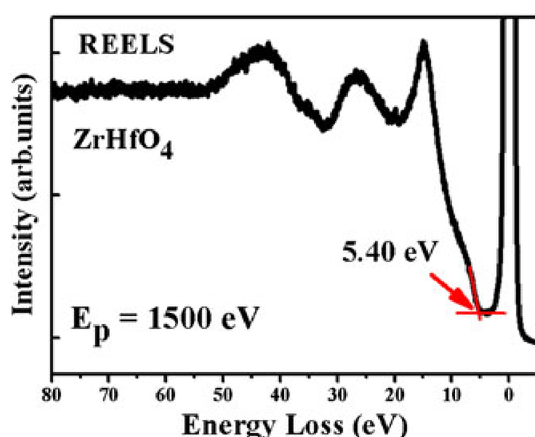

Figure 1. Reflection electron energy loss spectrum for $HfZrO_4$ thin film at the primary beam energy of 1500 eV.

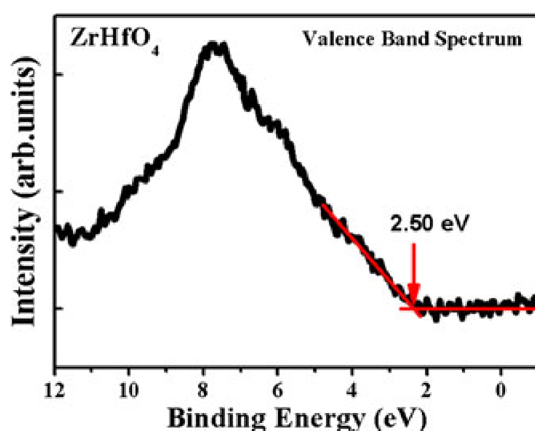

Figure 2. Valence band spectrum for $HfZrO_4$ thin film.

We also studied the optical properties of the $HfZrO_4$ thin films using the REELS spectra in conjunction with the Tougaard–Yubero QUEELS-ε(k,ω)-REELS software package.[9,10] The experimental inelastic scattering cross-section from the measured REELS spectrum is compared with that of the QUASES-XS-REELS software.[9] The procedure for a quantitative analysis of REELS has been described elsewhere.[4,6] The comparison between the theoretical and the experimental inelastic scattering cross-sections allows us to determine the dielectric function of the $HfZrO_4$ thin films. We define K_{exp} as the experimental cross-section and λ as the inelastic mean free path. The quantity of K_{exp} (ΔE) multiplied by λ is obtained by the multiple-scattering background subtracted from the measured REELS spectrum. The theoretical inelastic-scattering cross-section, K_{sc} multiplied by λ is then calculated using the dielectric response theory. Assuming that the inelastic process follows a Poisson distribution, then the single inelastic-scattering cross-section K_{sc} (E, ΔE) can be obtained from the effective inelastic-scattering cross-section averaged over all possible paths traveled by the electrons that have been inelastically scattered only once. In this model, the response of the material to a moving electron is described by the dielectric function ε, which is conveniently represented with the energy loss function (ELF) Im $(-1/\varepsilon)$. To estimate the ELF, we parameterized it as a sum of Drude–Lindhard type oscillators[9–11] given by

$$\text{Im}\left\{\frac{-1}{\varepsilon(\text{k},\omega)}\right\} = \theta(\hbar\omega - \text{E}_g)\cdot\sum_{i=1}^{n}\frac{A_i\gamma_i\hbar\omega}{\left(\hbar^2\omega_{0ik}^2 - \hbar^2\omega^2\right)^2 + \gamma_i{}^2\hbar^2\omega^2} \quad (2)$$

where the dispersion relation is given in the form

$$\hbar\omega_{0ik} = \hbar\omega_{0i} + \alpha_i\frac{\hbar^2k^2}{2m} \quad (3)$$

Here, A_i, γ_i and ω_i are the oscillator strength, the width, and the energy position of the *i*th oscillator, respectively, and $\hbar k$ is the momentum transferred from the REELS electron to the solid. The dependence of ω_{0ik} on k is generally unknown, but we can use Eqn (3) with α_i as an adjustable parameter. The step function $\theta(\hbar\omega - E_g)$ is included to describe the effect of energy band gap E_g in semiconductors and insulators. Here, $\theta(\hbar\omega - E_g) = 0$ if $\hbar\omega < E_g$ and $\theta(\hbar\omega - E_g) = 1$ if $\hbar\omega > E_g$. The band gap E_g, was estimated from the onset of the energy loss in the REELS data as shown in Fig. 1. The experimental inelastic cross-sections multiplied by λ after background subtraction were fitted with fitting parameters of the A_i, γ_i, $\hbar\omega_i$, and α_i, until good agreement with the calculated inelastic cross-section multiplied by λ at several primary electron energies is reached. The energy loss function Im $(-1/\varepsilon)$ is adjusted to make sure that it fulfills the well-established Kramers–Kronig sum rule,[9–11]

$$\frac{2}{\pi}\int_0^\infty \text{Im}\left\{\frac{1}{\varepsilon(\hbar\omega)}\right\}\frac{d(\hbar\omega)}{\hbar\omega} = 1 - \frac{1}{n^2} \quad (4)$$

Here, n is the index of refraction in the static limit. The index of refraction for $HfZrO_4$ is 1.8 (which is a weighted average for the

Copyright © 2012 John Wiley & Sons, Ltd.

refractive indices of HfO_2 and ZrO_2, and see also Ref. 12). The parameters in the ELF were determined through a trial-and-error procedure until the experimental and theoretical inelastic scattering cross-sections multiplied by λ are comparable. The parameters were determined from the REELS spectra for primary energies of 1.0, 1.5, and 1.8 keV.

Figure 3 shows the experimental and theoretical scattering cross-sections multiplied by λ as a function of energy loss at the primary energy of 1.0, 1.5, 1.8 keV. The plot shows that the experimental and theoretical results are in good agreement. The resulting oscillator parameters of the ELF for the $HfZrO_4$ thin film are tabulated in Table 1, which is in turn plotted in Fig. 4. Figure 4 shows the loss function Im $\{-1/\varepsilon\}$ and the corresponding surface energy loss function of the $HfZrO_4$ thin film for the energies ranging from 0 to 80 eV. As shown in Table 1 and Fig. 4, there are nine oscillators in the vicinity of 10.5, 15.6, 18.0, 21.5, 26.7, 34.5, 39.5, 46.5, and 57 eV for the ELF for $HfZrO_4$. The sharp energy loss peak at 15.6 eV may be interpreted as a collective excitation of the bound electrons. However, the oscillator strength correlated with the number of electrons contributed to the excitation, namely, the strength of the peak maximum around 26.7 eV. It indicates that the plasmon excitation is not exhausted at the energy around 15.6 eV and in fact the strength maximum around 26.7 eV is associated with a collective excitation of the entire valence band. The loss function, Im $\{-1/\varepsilon\}$ allows us to perform a Kramers–Kronig transformation to calculate the real part, Re $\{1/\varepsilon\}$ of the reciprocal of the complex dielectric functions. Thus, the real part ε_1 and the imaginary part ε_2 can be obtained using Im$\{-1/\varepsilon\}$ and Re$\{-1/\varepsilon\}$.[11]

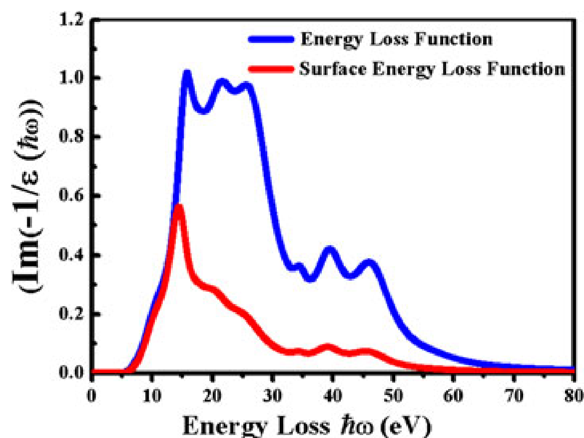

Figure 4. Energy loss function and surface energy loss function of $HfZrO_4$ thin film on Si(100) substrate.

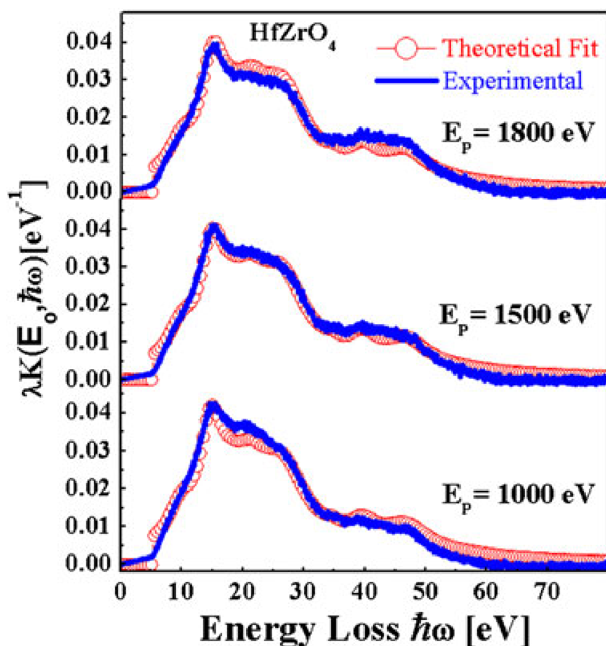

Figure 3. Experimental λk_{exp} for $HfZrO_4$ (red line) obtained from the REELS compared with theoretical λk_{th} (blue line) evaluated using the simulated energy loss function.

Table 1. Parameters used to model energy loss functions of $HfZrO_4$ thin films on *p*-Si (100) substrates that give the best fit to the experimental cross-sections at 1.0, 1.5, and 1.8 keV

	$\hbar\omega_{0i}$ (eV)	A_i (eV^2)	γ_i (eV)
$HfZrO_4$	10.5	5.89	5.0
($E_g = 5.40$)	15.6	31.30	3.3
($\alpha_i = 0.02$)	18.0	25.24	5.0
	21.5	72.70	6.5
	26.7	169.64	8.5
	34.5	6.56	2.5
	39.5	54.95	5.5
	46.5	110.09	8.0
	57.0	8.30	10.0

Figure 5 shows the values of the real part ε_1 and imaginary part ε_2 (corresponding to the absorption spectrum) of dielectric functions. These variations of ε_1 and ε_2 describe the insulating behavior well. The peak positions of the real part of dielectric function ε_1 at 7.7 eV and the imaginary part of dielectric function ε_2 at 8.9 eV indicate that the absorption is high at these frequencies. In the absorption spectrum described by ε_2, the strong absorption below 8.9 eV is associated with a transition of the valence band electrons into the unoccupied *d* states in the conduction band.[14,15]

The IMFP can be obtained from the ELF. The IMFP is highly important for the quantitative analysis of electron spectroscopy.

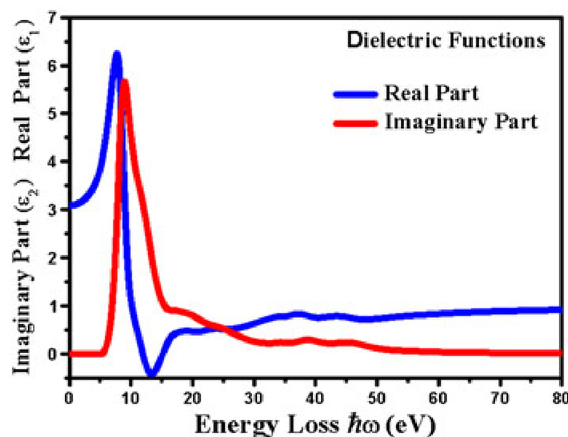

Figure 5. Optical properties of $HfZrO_4$ thin films. Real part (ε_1) and imaginary part (ε_2) of dielectric function.

Copyright © 2012 John Wiley & Sons, Ltd.

Figure 6 shows the theoretical inelastic scattering cross-section K_{sc} for the $HfZrO_4$ thin film at the primary beam energy of 1.0 and 1.8 keV. Inelastic electron scattering cross-section K_{sc} is related to the probability that the electron loses energy $\hbar\omega$ per unit energy loss and per unit path length traveled in the solid, and this includes the surface, bulk, and the interference excitation effects. Because of the interference effects, surface excitations cannot be separated from an experimental inelastic cross-section but can be approximately calculated individually from the following expression:[16,17]

$$K_S = \int (K_{sc} - K_{inf}) \mathrm{d}\hbar\omega, \qquad (5)$$

where K_s is the inelastic electron scattering cross-section because of the surface and K_{inf} is the inelastic electron scattering cross-section for electrons moving in an infinite medium because of bulk excitation. The inelastic electron scattering cross-sections K_{sc} and K_{inf} obtained by the QUEELS-ε(*k*,*ω*)-REELS software for $HfZrO_4$ gate dielectrics are shown in Fig. 6. As the primary beam energy increases, the inelastic cross-section generally decreases. As the primary energy is lowered, the value of K_s increases because the probability of the surface excitations is higher. In this work, we determined λ^{sc} and λ^{inf} from the inverse of the theoretically determined cross-section as defined in the form[6,16,17]

$$\lambda^{sc}(E_0) = \left[\int_0^\infty K_{sc}(E_0, \hbar\omega)\mathrm{d}\hbar\omega\right]^{-1} \text{ and}$$

$$\lambda^{inf}(E_0) = \left[\int_0^\infty K_{inf}(E_0, \hbar\omega)\mathrm{d}\hbar\omega\right]^{-1} \qquad (6)$$

Here, λ^{sc} is the IMFP estimated from the cross-section, which includes the surface, bulk, and the interference excitations, and λ^{inf} is the IMFP estimated from the cross-section of the bulk excitation. These IMFP values for $HfZrO_4$ thin films with the primary electron energy of 1.0, 1.5, and 1.8 keV are given in Table 2. The IMFP values for ZrO_2 thin films with the primary electron energies of 0.5, 1.0, 1.5, and 2.0 keV are also shown for comparison[6] with $\lambda_{TPP\text{-}2M}$ values, which are calculated from the Tanuma–Powell–Penn (TPP-2 M) formula [17]. As can be seen in Table 2, the λ^{sc} values for both ZrO_2 and $HfZrO_4$ are about 10–20% shorter than λ^{inf}. The λ^{inf} values for ZrO_2 are in good agreement with those of TPP-2 M, because TTP-2 M include only the bulk cross-section. The difference between the λ^{sc} and the λ^{inf} may be caused by the surface inelastic scattering cross-section, which is not included in the bulk value λ^{inf}. In any practical application of surface analysis by electron spectroscopy, the experimental IMFP values considering the surface inelastic scattering cross-section can be more useful. The IMFP estimated from the quantitative analysis of REELS provides a straightforward way to obtain the IMFP values for oxide thin films.

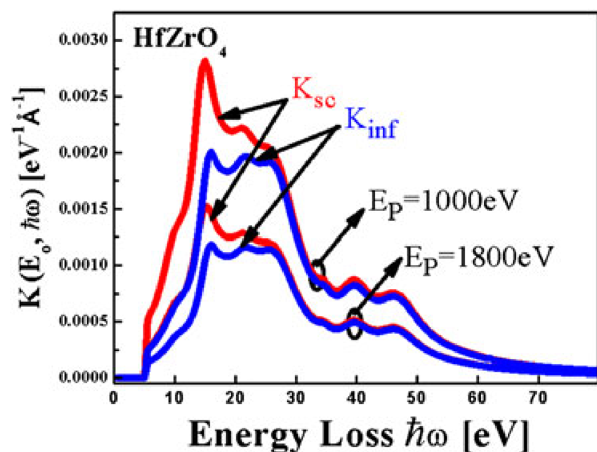

Figure 6. Inelastic electron scattering cros-sections K_{sc} and K_{inf} obtained by utilizing QUEELS-ε(*k*,*ω*)-REELS software for $HfZrO_4$ thin films at the primary energies of 1.0 keV and 1.8 keV.

Table 2. Inelastic mean free path (IMFP (Å)) of $HfZrO_4$ and ZrO_2[6] for primary energies from 1.0 to 1.8 keV determined in this paper

	$HfZrO_4$		ZrO_2		
E_0(eV)	λ^{sc}	λ^{inf}	λ^{sc}	λ^{inf}	$\lambda_{TPP\text{-}2M}$
500			7.6	9.6	11.3
1000	14.9	18.0	14.9	17.9	18.7
1500	22.0	25.9	22.0	25.8	25.5
1800	26.4	30.7			
2000			29.0	33.4	31.9

Conclusion

The band alignment of $HfZrO_4$ gate oxide thin film on Si was investigated using the REELS and XPS analysis. The band gap of $HfZrO_4$ gate oxide thin film is 5.40 ± 0.05 eV. The valence band offset (ΔE_v) and the conduction band offset (ΔE_c) are 2.5 ± 0.05 eV and 1.78 ± 0.05 eV, respectively. Our results meet the requirement of the hole and electron barrier heights of larger than 1 eV for device applications.

The optical properties and the inelastic mean free paths of $HfZrO_4$ gate oxide thin films were obtained by using a quantitative analysis of REELS spectra. REELS provides us a straightforward way to obtain the electronic and optical properties and the IMFP values for high-*k* gate oxide materials.

Acknowledgement

This work was supported by the Korea Research Foundation Grant funded by the Korean Government (MOEHRD, Basic Research Promotion Fund) (KRF-2008-313- C00225).

References

[1] R.F. Egerton, Electron Energy-Loss Spectroscopy in the Electron Microscopy (2nd edn), Plenum, New York, **1996**.
[2] H. Jin, S.K. Oh, H.J. Kang, S.W. Lee, Y.S. Lee, M.H. Cho, *Appl. Phys. Lett.* **2005**, *87*, 212902.
[3] H. Jin, S.K. Oh, H.J. Kang, M.H. Cho, *Appl. Phys. Lett.* **2006**, *89*, 122901.
[4] H. Jin, S.K. Oh, Y.J. Cho, H.J. Kang, S. Tougaard, *J. Appl. Phys.* **2007**, *102*, 053709.
[5] D. Tahir, E.K. Lee, S.K. Oh, T.T. Tham, H.J. Kang, H. Jin, S. Heo, J.C. Park, J.G. Chung, J.C. Lee, *Appl. Phys. Lett.* **2009**, *94*, 212902.
[6] D. Tahir, E.K. Lee, S.K. Oh, H.J. Kang, S. Heo, J.G. Chung, J.C. Lee, S. Tougaard, *J. Appl. Phys.* **2009**, *106*, 084108 .
[7] D.H. Triyoso, G. Spencer, R.I. Hedge, R. Gregory, X.D. Wang, *Appl. Phys. Lett.* **2008**, *92*, 113501 .
[8] W. Keren, *RCA Rev.* **1970**, *31*, 207.
[9] S. Tougaard, F. Yubero, QUEELS-ε(k, ω)-REELS: Software Package for Quantitative Analysis of Electron Energy Loss Spectra; Dielectric

Copyright © 2012 John Wiley & Sons, Ltd.

Function Determined by Reflection Electron Energy Loss Spectroscopy. Version 3.0, **2008**. See http://www.quases.com
[10] F. Yubero, J.M. Sanz, B. Ramskov, S. Tougaard, Phys. Rev., **1996**, *B53*, 9719.
[11] F. Wooten, Optical Properties of Solid, Academic, New York, **1972**
[12] www.luxpop.com.
[13] L.K. Dash, N. Vast, P. Baranek, M.C. Cheynet, L. Reining, *Phys. Rev.* **2004**, *B70*, 245116.
[14] D.W. McComb, *Phys. Rev.* **1996**, *B54*, 10.
[15] N. Pauly, S. Tougaard, *Surf. Interf. Anal.* **2008**, 40, 731
[16] N. Pauly, S. Tougaard, *Surf. Sci.* **2008**, *602*, 1974.
[17] S. Tanuma, C.J. Powell, D.R. Penn, *Surf. Interf. Anal.* **1994**, *21*, 165.

 Copyright © 2012 John Wiley & Sons, Ltd.